

This article was downloaded by:

On: 25 January 2011

Access details: *Access Details: Free Access*

Publisher *Taylor & Francis*

Informa Ltd Registered in England and Wales Registered Number: 1072954 Registered office: Mortimer House, 37-41 Mortimer Street, London W1T 3JH, UK



Journal of Wood Chemistry and Technology

Publication details, including instructions for authors and subscription information:

<http://www.informaworld.com/smpp/title~content=t713597282>

Surface Porosity of Lignin/PP Blend Carbon Fibers

Satoshi Kubo^{ab}, Takahiro Yoshida^c, John F. Kadla^a

^a Faculty of Forestry, Department of Wood Science, University of British Columbia, Vancouver, BC, Canada ^b Department of Biomass Chemistry, Forest and Forest Products Research Institute, Tsukuba, Ibaraki, Japan ^c Department of Wood Processing, Forestry and Forest Products Research Institute, Tsukuba, Ibaraki, Japan

Online publication date: 04 December 2010

To cite this Article Kubo, Satoshi, Yoshida, Takahiro and Kadla, John F. (2007) 'Surface Porosity of Lignin/PP Blend Carbon Fibers', *Journal of Wood Chemistry and Technology*, 27: 3, 257 – 271

To link to this Article: DOI: 10.1080/02773810701702238

URL: <http://dx.doi.org/10.1080/02773810701702238>

PLEASE SCROLL DOWN FOR ARTICLE

Full terms and conditions of use: <http://www.informaworld.com/terms-and-conditions-of-access.pdf>

This article may be used for research, teaching and private study purposes. Any substantial or systematic reproduction, re-distribution, re-selling, loan or sub-licensing, systematic supply or distribution in any form to anyone is expressly forbidden.

The publisher does not give any warranty express or implied or make any representation that the contents will be complete or accurate or up to date. The accuracy of any instructions, formulae and drug doses should be independently verified with primary sources. The publisher shall not be liable for any loss, actions, claims, proceedings, demand or costs or damages whatsoever or howsoever caused arising directly or indirectly in connection with or arising out of the use of this material.

Surface Porosity of Lignin/PP Blend Carbon Fibers

Satoshi Kubo

Faculty of Forestry, Department of Wood Science, University of British
Columbia, Vancouver, BC, Canada and Department of Biomass
Chemistry, Forest and Forest Products Research Institute, Tsukuba,
Ibaraki, Japan

Takahiro Yoshida

Department of Wood Processing, Forestry and Forest Products Research
Institute, Tsukuba, Ibaraki, Japan

John F. Kadla

Faculty of Forestry, Department of Wood Science, University of British
Columbia, Vancouver, BC, Canada

Abstract: The surface porosities of carbon fibers derived from the polymer blend fibers of hardwood kraft lignin, HKL and polypropylene, PP, were discussed using thermal analyses, FTIR, and nitrogen adsorption. HKL/PP carbon fibers were prepared by two-step thermal processing, thermostabilization, and carbonization. During the thermostabilization process, pores are created by oxidative degradation of the PP component. After thermostabilization some crystalline and highly oxidized PP components remained in the blend fiber. These residual PP components were subsequently pyrolyzed during carbonization, and effectively created a porous structure in the resulting carbon fibers. N₂ adsorption tests of the porous carbon fibers revealed the same type of adsorption/desorption isotherms as for activated carbon fiber. The internal surface area of the HKL/PP = 62.5/37.5 carbon fibers was calculated to be 499 m² g⁻¹. This value was lower than that for commercial activated carbon,

The authors acknowledge UBC and FFPRI for financial support of this research. The authors also acknowledge R. A. Venditti and R. D. Gilbert for their discussion for this research.

Address correspondence to John F. Kadla, Faculty of Forestry, Department of Wood Science, University of British Columbia, 2424 Main Mall, Vancouver, BC, V6T 1Z4, Canada. E-mail: john.kadla@ubc.ca

745 m² g⁻¹. However, these porous lignin-based carbon fibers were not activated carbon fibers, which could be relatively easily done through steam activation. Thus, the HKL/PP blend carbon fibers appear to be promising precursors for activated carbon fibers.

Keywords: Lignin, polymer blend, porous carbon fiber

INTRODUCTION

Lignin is one of the most abundant natural polymers. It is produced in the chemical pulping industry as by-products, used for energy generation and recovery of pulping chemicals. This recovering system is one of the most well-established processes for the utilization of biomass as a fuel. Today, modern recovery systems have high heat recovery efficiencies and are able to meet the energy demands of a conventional pulp mill. As a fuel, lignin has a lower standard heat of combustion (12.6 MJ kg⁻¹, as dry black liquor^[1]) than other fuels, such as coal (~25 MJ kg⁻¹), heavy oil (~40 MJ L⁻¹), and natural gas (~35 MJ L⁻¹). As a result, extensive research and development has been conducted to improve the efficiency and recovery of heat and energy from lignin, and new conversion systems have been developed (e.g., gasification).^[2] These developments will make it possible to provide surplus lignin for other value-added applications outside of chemical recovery and energy generation. Some lignin recovering processes have been examined to produce value-added lignin products for both fuel^[3] and materials applications.^[4] Moreover, large amounts of lignins will be generated as part future wood-to-ethanol bio-refineries. In these systems, the development of value-added lignin-based products will be paramount to the economic success of the bio-ethanol production.

In our previous work, industrial lignin preparations were converted into fibrous materials by simple thermal treatment and/or polymer blending methods followed by thermal spinning.^[5-7] These lignin fibers were transformed into carbon fibers using a thermal conversion process similar to that found in industry. Mechanical properties of these carbon fibers were comparable to industrial general performance (GP) grade carbon fibers prepared from isotropic pitch.^[8] Depending on the blending polymer, porous lignin-based fibers could be prepared.^[9] Carbonization of the immiscible polymer blend fibers produced porous/hollow carbon fibers without any additional activation (Figure 1). Mechanical properties were inferior to other lignin-based carbon fibers having smooth surfaces. However, tensile strengths of these porous fibers were 167-332 MPa, depending on the blending ratio. These tensile strengths were comparable to, or higher than that for commercial pitch-based activated carbon fibers. However, for commercial viability, the surface area of the lignin-based porous carbon fibers must be comparable to activated carbons. In this study, nitrogen adsorption tests were performed to

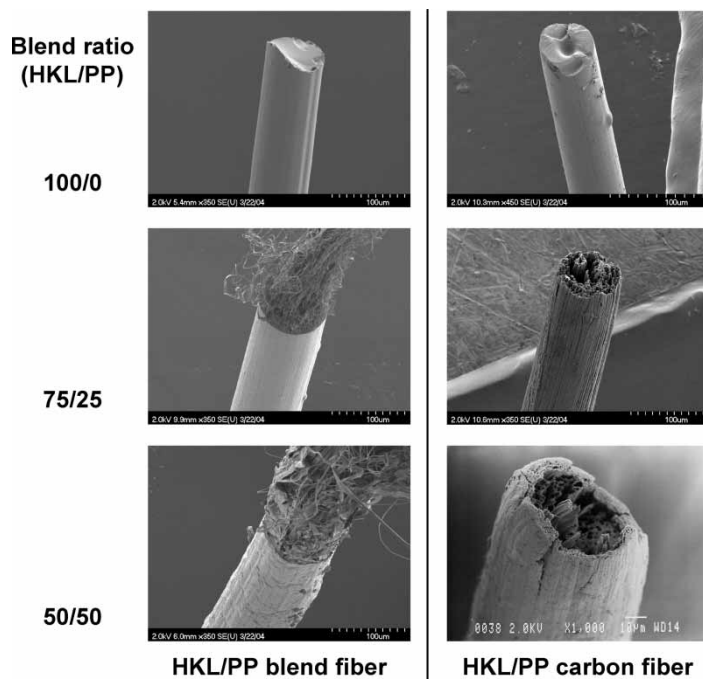


Figure 1. Scanning electron micrograms of HKL/PP blend fibers and the corresponding carbon fibers.

estimate the porosity and mechanism of pore creation in lignin-based porous carbon fiber.

EXPERIMENTAL

Preparation of Carbon Fibers

Hardwood kraft lignin (HKL) was obtained from Westvaco Corp, SC, USA. The HKL was repeatedly washed with dilute HCl (pH 2) to removed inorganic impurities, and improve thermal fiber spinning. Isotactic PP with a melt index of 35 was purchased from Aldrich chemicals. HKL/PP blends were prepared as previously reported,^[9] and thermally spun into fibers using an Atlas Laboratory Mixing Extruder (Atlas Corp.). The spinning temperature of the HKL and all blend samples was adjusted between ca. 210–220°C. Blended fibers were oxidized at 250°C for 1 h under an air atmosphere prior to carbonization to change the thermoplastic nature of the HKL/PP blend fibers. The oxidized (thermostabilized) fibers were then carbonized under a

nitrogen flow at 1,000°C for 1 h. The heating rates employed for oxidation (thermostabilization) and carbonized were 18 and 180°C h⁻¹, respectively.

Surface Characterization of Carbon Fibers

N₂ gas adsorption analysis was performed using a BELSORP 18 (Bel Japan, Inc.) at 77 K. Carbonized and thermostabilized fibers were completely dried before analysis at 250°C for 15 h and 110°C for 24 h under reduced pressure in the sample cell, respectively. Specific surface area was calculated by the BET multi-point method. Internal surface area was calculated from the BET specific surface measurements combined with the t-method, to estimate the ratio of internal to external surface area. Commercial powdered activated carbon (Column chromatograph grade, Wako Pure Chemicals, Japan) was used as a comparison sample for surface area measurements.

General Analysis

Differential scanning calorimetric, DSC, analyses were performed using a TA Instruments Q1000 DSC under a nitrogen flow. The temperature was scanned from -80 to 250°C with a heating rate of 20°C min⁻¹. The second heating run was used to determine the glass transition temperature, T_g, and the melting temperature, T_m. A TA Instruments Q500 TGA and Shimadzu DTG-60 were used for thermogravimetric analyses, TGA, and differential thermal analysis, DTA, respectively. Both analyses were performed using Ultra pure grade N₂ gas. Scanning electron microscopy (SEM) was run on gold-coated fibers using a HITACHI S-4700 Scanning Electron Microscope with an accelerating voltage of 2 kV. Diffuse reflectance method was employed for FTIR analysis. FTIR spectra were recorded using a Perkin Elmer Spectrum 2000. A total of 128 scans were acquired at a spectral resolution of 4 cm⁻¹. All spectra were corrected with Kubelka-Munk conversion.

RESULT AND DISCUSSION

Thermal Decomposition of HKL/PP Fibers During the Thermostabilization Process

The production of carbon fibers, generally, involves two different thermal conversion processes, thermostabilization and carbonization. Typically, precursor fibers are thermostabilized by heating in air or oxidizing gas prior to carbonization, which is typically performed in an ambient atmosphere at high temperature.^[10] In our previous research,^[11] various types of pores were observed under SEM analysis for the surface of carbonized lignin/PP blend fibers.

However, SEM analysis of the thermostabilized fibers also revealed some morphological changes in the fiber surface (Figure 2). TGA curves of HKL/PP blend fibers are shown in Figure 3(A). Thermal decomposition of the HKL/PP blend fibers contained two different decomposition steps; the weight loss at lower and higher temperature being mainly related to the thermal decomposition of HKL and PP components, respectively. It can be seen that the blend ratio is maintained through the spinning process despite phase separation. The 50/50 HKL/PP blend fiber has a final residual weight of $\sim 21\%$ as compared to the 100% HKL fiber at $\sim 42\%$ residue.

The change in weight of the HKL/PP blend fibers during the thermostabilization process was monitored using TGA. Figure 4 shows the change in fiber weight as temperature is increased from 100°C to 250°C with increasing PP contents. In air (Figure 4(A)), only 9.0% weight loss was detected after heating the pure HKL fiber to 250°C , whereas for the 50/50 HKL/PP blend fiber a 46.2% weight loss was observed (Table 1). The pure PP fiber had an almost 80% reduction in weight after thermostabilization. Therefore, the observed differences in weight changes between the pure HKL and HKL/PP blend fibers are due to the incorporation of the PP component into the HKL matrix. By contrast, under a nitrogen atmosphere, the extent of weight loss of the various HKL/PP fibers was substantially less

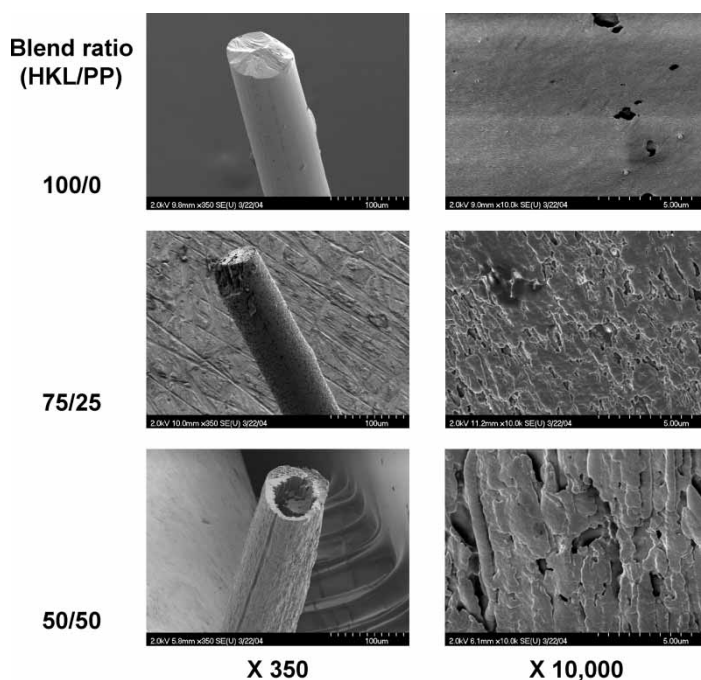


Figure 2. Scanning electron micrograms of thermostabilized HKL/PP blend fibers.

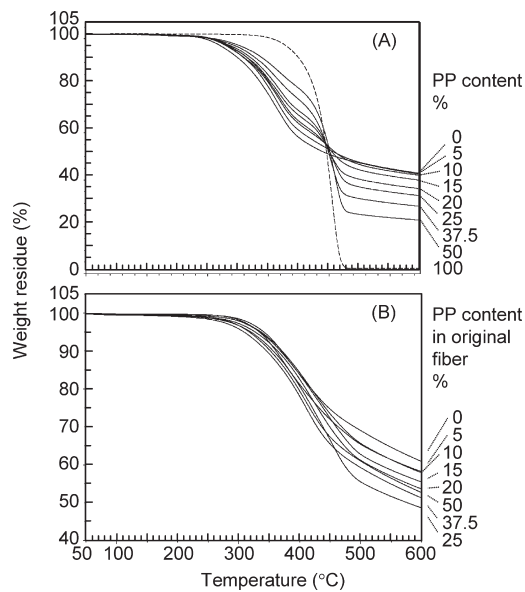


Figure 3. TGA curves of HKL/PP (A) blend fibers, and (B) thermostabilized fibers.

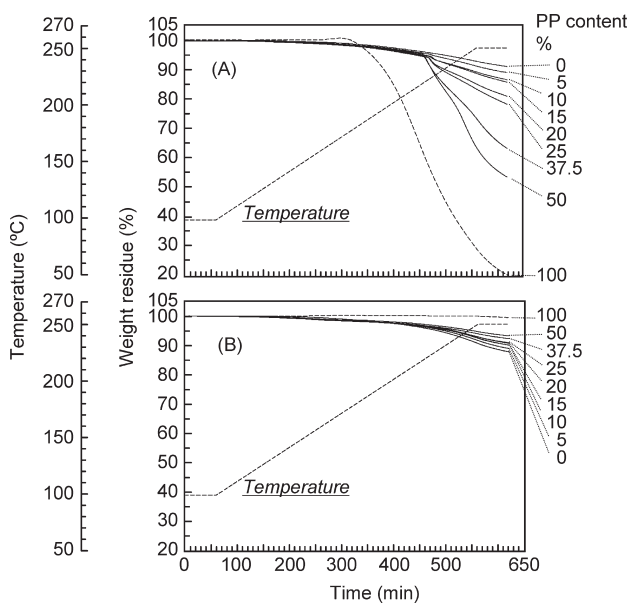


Figure 4. Weight change of HKL/PP blend fibers during thermal processing under thermostabilization conditions in (A) Air and (B) N₂ atmospheres.

Table 1. Thermal decomposition of HKL/PP fibers during the thermostabilization in air and N₂ atmospheres

Blend fiber HKL/PP	Under air (thermostabilization)			Under N ₂ Weight loss (%) ^a
	Weight loss (%) ^a	Decompo- sition temp- erature (°C) ^b	DTA-peak- top tempera- ture (°C)	
100/0	9.0	230	—	12.6
95/5	11.0	223	220	11.3
90/10	13.5	224	217	10.0
85/15	14.2	224	218	10.2
80/20	19.0	223	215	9.4
75/25	21.7	223	215	9.3
63/37	36.6	220	214	7.8
50/50	46.3	220	215	6.9
0/100	79.2	190	—	0.5

^aMeasured after heating to 250°C.

^bMeasured as inflection point temperature.

(Figure 4(B)). Under anaerobic conditions (N₂ atmosphere), the pure PP fiber was thermally stable over the temperature range studied; the thermal decomposition was less than 1%. This result suggests that the PP component is oxidatively decomposed during the thermostabilization process (i.e., in air). Under anaerobic conditions, the temperatures at which the HKL/PP blend fibers decompose increases with increasing PP content (Table 1). The residual weight of the 50/50 HKL/PP blend fiber was higher than that of the pure HKL fiber.

Figure 4(A) also illustrates that PP fiber decomposition in air is initiated at 197°C (5% weight loss), much lower than that observed for the HKL/PP blend fibers (~220°C, inflection point temperature). DTA analysis of the HKL/PP blend fibers (Figure 5) revealed an exothermic peak, assigned to oxidation of the PP component.^[12] The temperature of the exothermic peak is comparable to that obtained from TGA, and follows the same trend. Increasing PP content leads to a slight decrease in temperature (Table 1), but it is well above that expected for the PP component. The blending of lignin with the PP changes the decomposition of PP, likely due to lignin acting as an anti-oxidant for PP.^[13]

Interestingly, decomposition of the pure HKL fibers occurred more significantly under anaerobic conditions than under aerobic conditions, 12.6% versus 9% weight loss, respectively. During the thermal processing of pure HKL fibers under aerobic conditions, oxidation occurs and oxygen atoms are introduced into lignin molecular structure.^[14] Likewise, the PP fiber also appeared to undergo oxygenation with a weight increase at ~172°C, but rapidly underwent oxidative decomposition at higher temperatures. The extensive oxidative decomposition of the pure PP fiber as compared with oxygenation,

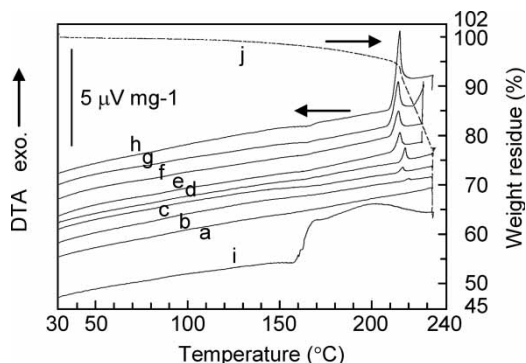


Figure 5. DTA curves of HKL/PP blend fibers measured under thermostabilization condition. HKL/PP: (a) 100/0, (b) 95/5, (c) 90/10, (d) 85/15, (e) 80/20, (f) 75/25, (g) 62.5/37.5, (h) 50/50, (i) 0/100. (j) Thermal decomposition curve of the 50/50 HKL/PP fiber measured by DTA.

explains the low yield of the PP rich blend fibers after the thermostabilization process. It is believed that this oxidative decomposition of the PP component results in the creation of pores in the thermostabilized HKL/PP blend fibers.

The specific surface area of the thermostabilized HKL/PP blend fibers were estimated by N_2 adsorption at 77 K. The adsorption/desorption isotherms of the various HKL/PP blend thermostabilized fibers are shown in Figure 6. Although SEM observed various sizes of pores, the effective

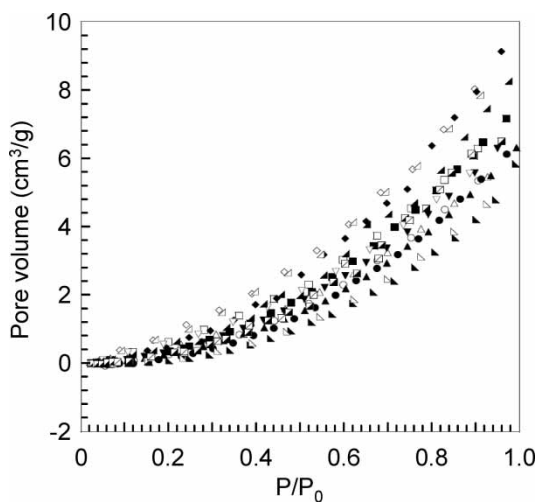


Figure 6. N_2 adsorption/desorption isotherms of thermostabilized HKL/PP fibers. HKL/PP: 100/0(●), 95/5(■), 90/10(◆), 85/15(▲), 80/20(▼), 75/25(▾), 62.5/37.5(▴), 50/50(▣)

surface area could not be calculated. When the thermostabilized fibers were dried for N₂ adsorption analysis a char-like material was generated, even when low temperature, 110°C, was employed. Deposition of these char like materials on the fiber surfaces will impact the estimation of the specific surface areas. Therefore, to confirm the availability of the surface pores other analytical methods will be required, which can prevent the thermal decomposition of fiber components.

Structure of Residual PP Components in Thermostabilized Fibers

The TGA curves of the thermostabilized HKL/PP blend fibers (Figure 3(B)) are considerably different from those for the original HKL/PP blend fibers (Figure 3(A)). The thermal decomposition of the thermostabilized blend fibers appears as a one-step process, and the residue weight values at 600°C were not consistent with the original blend compositions. This result might indicate that some PP components remain in the thermostabilized fibers, but are no longer proportional to the original blend compositions.

DSC analysis of the HKL/PP blend fibers and corresponding thermostabilized fibers are shown in Figure 7. The HKL/PP blend fibers contained two T_g's at the same temperature range as the pure HKL and PP fibers: consistent with the immiscible nature of this blend.^[9] However, the T_g assigned to the HKL component was not detected in the thermostabilized fibers. This indicates that in all of these fibers the HKL component was thermostabilized under these conditions.

The melting peak of the PP component in the original HKL/PP blend fibers appeared at 162–163°C for all samples (as peak top temperature). The melting peak area of the PP component has a good correlation with PP content, and indicates that the degree of crystallinity of the PP component was not affected by the HKL content (Figure 8). By contrast, no correlation between the melting peak area and blend compositions was observed for the thermostabilized fibers. In fact, the melting peak of the PP component was not observed in the 95/5 and 50/50 HKL/PP thermostabilized fibers. However, those fibers will contain PP. (From the data shown in Table 1, at least 21% of PP will remain in the blend fibers.) Therefore, these observations might indicate that under the oxidizing conditions of the thermostabilization process, the melting-crystallizing process changed the degree of crystallinity of the PP component.

To estimate the residual PP content, FTIR analysis was performed on the thermostabilized fibers. The thermostabilized, oxidized HKL/PP fibers are black colored hard materials. This makes it difficult to collect clear FTIR spectrum for some samples. For this reason, diffuse reflectance method with Kubelka-Munk conversion was employed. Diffuse reflectance FTIR gave clear spectra for all of the oxidized

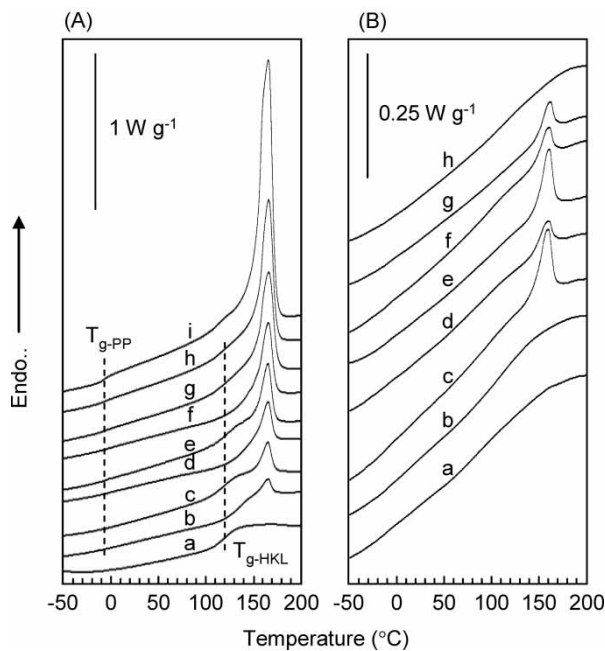


Figure 7. DSC curves of (A) HKL/PP blend fibers and (B) corresponding thermostabilized fibers. HKL/PP: (a) 100/0, (b) 95/5, (c) 90/10, (d) 85/15, (e) 80/20, (f) 75/25, (g) 62.5/37.5, (h) 50/50, (i) 0/100.

HKL/PP fibers. As shown in Figure 9, the intensity of the C-H stretching bands ($\nu_{\text{C-H}} = \sim 2,800\text{--}3,100\text{ cm}^{-1}$), which will be more related with the PP component than the HKL, increased proportionally with increasing PP content. This observation indicates that the PP content in the

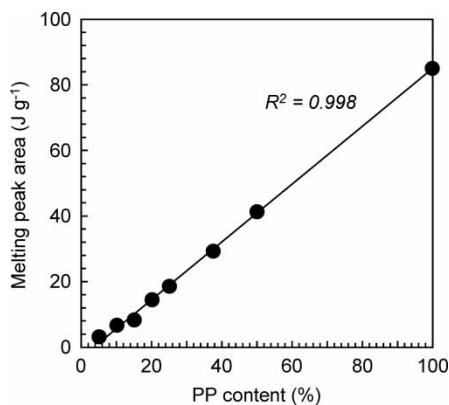


Figure 8. Relationship between melting peak area and PP content.

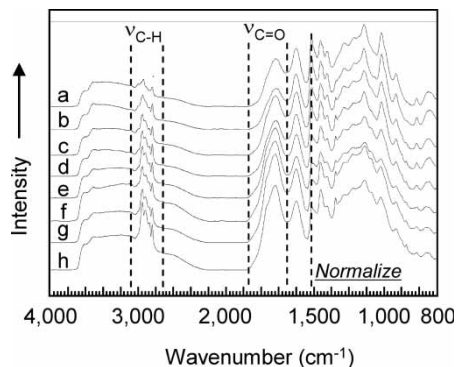


Figure 9. FTIR spectra of thermostabilized HKL/PP fibers. HKL/PP: (a) 100/0, (b) 95/5, (c) 90/10, (d) 85/15, (e) 80/20, (f) 75/25, (g) 62.5/37.5, (h) 50/50.

thermostabilized fibers derived from originally PP rich HKL/PP fibers (e.g., 50/50 HKL/PP) were higher than those from HKL rich fibers. Thus, in the 50/50 HKL/PP thermostabilized fibers the PP component remains as an amorphous phase.

Another characteristic FTIR band of the thermostabilized blend fibers was observed at the C=O stretching ($\nu_{\text{C=O}}$) region. The intensity for $\nu_{\text{C=O}}$ band was higher in the PP rich blend fibers as compared to the pure HKL fiber. This suggests that nonvolatile oxidized PP components exist in the thermostabilized blend fibers. Together, these results indicate that the composition of the PP related structures, including both intact and oxidized structures, are higher in the thermostabilized fibers derived from PP rich blends as compared with those from HKL rich blends. The thermal properties, such as thermal decomposition and thermal transition temperatures, of oxidized PP are most likely different from that of non-oxidized PP. This difference explains the discrepancy between the quantitative analysis of PP components in the original fibers and the thermostabilized fibers using DSC and TGA.

Surface Properties of HKL/PP Blend Carbon Fibers

In our previous research, it was presumed that the surface pores on the HKL/PP blend carbon fibers was created by the pyrolysis of the PP component during the high temperature thermal processing. DTA curves of thermostabilized HKL/PP fibers are shown in Figure 10. Although all of the curves exhibit a broad rolling baseline at low temperatures, no specific peaks were observed in the DTA curves at temperatures lower than 400°C. In the temperature range between 400 and 500°C, a broad endothermic peak was detected in all of the thermostabilized HKL/PP blend fibers. This broad endothermic peak

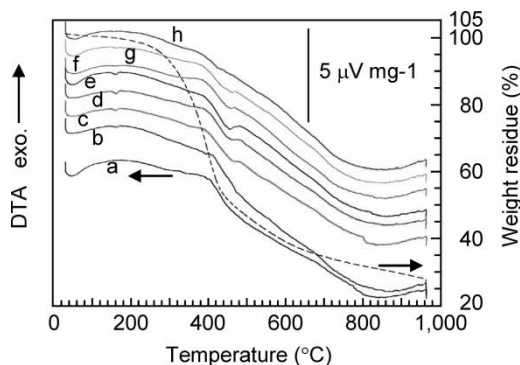


Figure 10. DTA curves of the thermostabilized HKL/PP fibers measured under carbonization conditions. HKL/PP: (a) 100/0, (b) 95/5, (c) 90/10, (d) 85/15, (e) 80/20, (f) 75/25, (g) 62.5/37.5, (h) 50/50, (i) 0/100, and (j) Thermal decomposition curve of the thermostabilized 50/50 HKL/PP fiber as measured by DTA.

can be assigned to the thermal decomposition of the PP component (this temperature range is consistent with the thermal decomposition of PP fibers as shown in Figure 3(A)), which is expected to create pores in the HKL/PP blend carbon fibers. However, this broad peak was not observed in the 50/50 HKL/PP thermostabilized fibers. The non-oxidized PP content in the 50/50 HKL/PP thermostabilized fibers might be very low, lower than the detection level of DTA analysis, and most of PP might be present in an oxidized form. In the high temperature region ($>500^{\circ}\text{C}$) the DTA curve gradually shifted to the endothermic direction. This likely corresponds to thermal decomposition and molecular reorganization of the HKL component. However, like the low temperature region, no observable peaks were found over this high temperature range. It is likely that the molecular structure of the oxidized PP components varies in the thermostabilized blend fibers, and may preclude the detection of the specific thermal decomposition of the oxidized PP by DTA analysis.

The specific surface area of the HKL/PP blend carbon fibers were estimated by N_2 adsorption. Adsorption/desorption isotherms and BET surface areas are shown in Figure 11 and Table 2, respectively. N_2 adsorption increased rapidly at low relative pressure, and no hysteresis loop was observed in the middle pressure range. The profiles of these isotherms indicates the formation of micropores in the HKL/PP blend carbon fibers,^[15] but no significant amount of mesopores. This is consistent with that observed for the activated carbon fiber.^[16] However, the calculated specific surface areas of these carbon fibers are lower than that of commercial activated carbons. Furthermore, the BET surface area calculated for the pure HKL carbon fiber, internal surface area = $331\text{ m}^2\text{ g}^{-1}$, was higher than those for carbon fibers prepared from HKL rich blend fibers. It is possible that gasses generated by

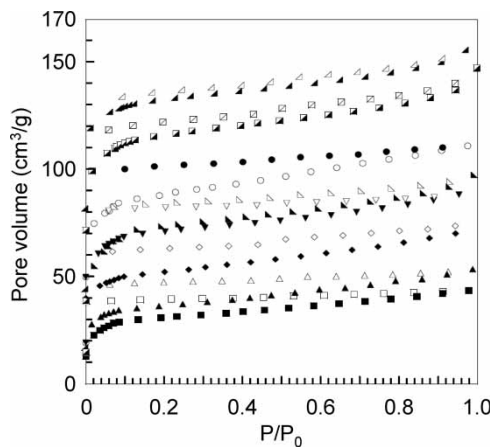


Figure 11. N₂ adsorption/desorption isotherms of HKL/PP carbon fibers. HKL/PP: 100/0(●), 95/5(■), 90/10(◆), 85/15(▲), 80/20(▼), 75/25(◄), 62.5/37.5(►), 50/50(◩).

the thermal treatment of PP and PP related components will react and end up as carbonized structures, filling fine pores in the carbon fibers. As described earlier, the thermostabilized fibers contained some char-like materials, which could have adsorbed onto the surface and/or inside pores of the thermostabilized fibers. These char-like materials might be favorably generated from the PP component as compared to the HKL. In our previous report, the carbonization yield of 95/5 HKL/PP blend fibers, 53.2%, was slightly higher than that of pure HKL fibers, 51.6%.^[9] Moreover, carbonization yield was not significantly decreased by blending with 12.5% of PP, 50.5%. By contrast, some large pores might be created in the PP rich blend fibers before the

Table 2. Pore volume of thermal treated HKL/PP blend fibers at 1,000°C

Blend fiber HKL/PP	Specific surface area (m ² /g)	Internal surface area (m ² /g)
100/0	336	331
95/5	117	114
90/10	197	180
85/15	139	135
80/20	270	257
75/25	271	263
63/37	512	499
50/50	444	433
Commercial activated carbon, powder	880	745

carbonization process; hollow shaped fibers were prepared from PP rich fibers by thermostabilization (Figure 1). The large sized pores will help in the transportation of pyrolysis gases from the inside of fibers.^[17] In the high PP content blends a significant amount of pyrolysis gas would be created, which would destroy fine pores and lead to mesopore creation, and also decrease the amount of internal surface area of the carbon fibers. In fact, the adsorption/desorption isotherm of the 50/50 HKL/PP blend carbon fibers showed a trace of a hysteresis loop in the middle pressure range, and the N₂ adsorption was slightly increased at high relative pressure, which would indicate the formation of some mesopores and macropores, respectively.

Although, these fibers had low BET surface areas as compared to commercial activated carbon, these porous lignin carbon fibers could be easily activated with relatively simple processes, for example, steam activation. In fact, lignin-based carbon fibers prepared from softwood acetic acid lignin with a BET surface area of 370 m² g⁻¹, and lower tensile strength, < 150 MPa, were converted into excellent activated carbon fibers with large surface area and high tensile strength.^[18] Thus, the HKL/PP carbon fibers, which have higher tensile strength and larger surface area than the acetic acid lignin-based carbon fibers may also be converted into good activated carbon fibers using the same activation process.

CONCLUSION

Porous carbon fibers were produced from immiscible polymer blends of HKL and PP. Pore creation occurred by a two-step process; oxidative degradation of the PP component followed by pyrolysis gasification of residual PP related components. Within these processes, gasification would be the main factor for pore growth. Effective pore volumes calculated by N₂ adsorption were lower than that for commercial activated carbons. However, relatively simple processes, such as steam activation, could effectively activate these porous lignin carbon fibers and make them suitable for commercial applications.

REFERENCES

1. General Policy Planning Division of Agency for Natural Resources and Energy (ANRE), Japan. *Standard chart of heat of combustion values for energies*; May. 2007. Available at <http://www.enecho.meti.go.jp/info/statistics/energy/070525hatsunetsu.pdf>.
2. Larsson, A.; Nordin, A.; Backman, R.; Warnqvist, B.; Eriksson, G. Influence of black liquor variability, combustion, and gasification process variables and inaccuracies in thermochemical data on equilibrium modeling results. *Energy Fuels* **2006**, *20*, 359–363.
3. Tonami, P. LignoBoost does business with lignin fuel. *Beyond Magazine* **2007**, 4–5.

4. Brodin, I.; Gellerstedt, G.; Sjöholm, E. Kraft lignin as feedstock for chemical products. In *Proceeding CD of 14th International Symposium on Wood, Fiber and Pulpinc Chemistry*. Durban, South Africa, 2007, Proceeding ID:114.
5. Kadla, J.F.; Kubo, S.; Venditti, R.; Gilbert, R.; Compere, A.; Griffith, W. Lignin-based carbon fibers for composite fiber applications. *Carbon* **2002**, *40*, 2913–2920.
6. Kubo, S.; Gilbert, R.D.; Kadla, J.F. Lignin-based polymer blends and biocomposite materials. In *Natural Fibers, Biopolymers and their Biocomposites*; Mohanty, A.K., Misra, M., and Drzal, L.T. Eds.; CRC Press, 2004, 671–698.
7. Kadla, J.F.; Kubo, S. Lignin-based polymer blends: Analysis of intermolecular interactions in lignin-synthetic polymer blends. *Composites, Part A: Applied Science and Manufacturing* **2004**, *35* (3), 395–400.
8. Kubo, S.; Kadla, J.F. Lignin-based carbon fibers: Effect of synthetic polymer blending on fiber properties. *J. Polym. Environ.* **2005**, *13*, 97–105.
9. Kadla, J.F.; Kubo, S.; Venditti, R.; Gilbert, R. Novel hollow core fibers prepared from lignin polypropylene blends. *J. Appl. Polym. Sci.* **2002**, *85*, 1353–1355.
10. Otani, S. Precursors and productions of carbon fibers. Otani, S., Okuda, K., and Matsuda, H., Eds. In *Carbon Fibers*; Kindai Henshu: Tokyo, Japan, 1983, 101–169.
11. Kadla, J.F.; Kubo, S. Carbon fibers from lignin-recyclable plastic blends. In *Encyclopedia of Chemical Processing*; Cohen, A. Ed.; Marcel Dekker, Inc.: New York, NY, 2005, 317–331.
12. Kaloustian, J.; Antonetti, P.; Berrada, A.; Claire, Y.; Perichaud, A. Thermal behavior of polypropylene during aging. *J. Therm. Anal. Calorim.* **1998**, *52*, 327–340.
13. Pouteau, C.; Dole, P.; Cathala, B.; Averous, L.; Boquillon, N. Antioxidant properties of lignin in polypropylene. *Polym. Degrad. Stabil.* **2003**, *81*, 9–18.
14. Braun, J.; Holtman, K.; Kadla, J. Lignin-based carbon fibers: oxidative thermostabilization of kraft lignin. *Carbon* **2005**, *43*, 385–394.
15. Brunauer, S.; Deming, L.; Deming, W.; Teller, E. On a theory of the van der Waals adsorption of gases. *J. Am. Chem. Sci.* **1940**, *62*, 1723–17320.
16. Yang, O.; Kim, J.; Lee, J.; Kim, Y. Use of activated carbon fiber for direct removal of iodine from acetic acid solution. *Ind. Eng. Chem. Res.* **1993**, *32*, 1692–1697.
17. Juntgen, H. New applications for carbonaceous adsorbents. *Carbon* **1977**, *15*, 273–283.
18. Uraki, Y.; Nakatani, A.; Kubo, S.; Sano, Y. Preparation of activated carbon fibers with large specific surface area from softwood acetic acid lignin. *J. Wood Sci.* **2001**, *47*, 465–469.